An inexpensive, versatile, compact, programmable temperature controller and thermocycler for simultaneous analysis and visualization within a microscope

Pablo Martínez Cruz[1], Mikayla Wood[1], Reha Abbasi[1,2], Thomas B. LeFevre[1,2], Stephanie E. McCalla[1]*

[1] Chemical and Biological Engineering Department, Montana State University, PO Box 173920, Bozeman, MT, 59717, United States of America

[2] Center for Biofilm Engineering, Montana State University, PO Box 173980, Bozeman, MT, 59717, United States of America

*Corresponding author email: stephanie.mccalla@montana.edu

ABSTRACT: Microfluidic Lab on a Chip (LOC) devices are key enabling technologies for research and industry due to their compact size, which increases the number of integrated operations while decreasing reagent use. Common operations within these devices such as chemical and biological reactions, cell growth, or kinetic measurements often require temperature control. Commercial temperature controllers are constrained by cost, complexity, size, and especially versatility for use in a broad range of applications. Small companies and research groups need temperature control systems that are more accessible, which have a wide applicability. This work describes the fabrication and validation of an inexpensive, modular, compact, and user-friendly temperature control system that functions within a microscope. This system provides precise temperature acquisition and control during imaging of any arbitrary sample which complies with the size of a microscope slide. The system includes two parts. The first part is a compact and washable Device Holder that is fabricated from high temperature resistant material and can fit securely inside a microscope stage. The second part is a robust Control Device that incorporates all the necessary components to program the temperature settings on the device and to output temperature data. The system can achieve heating and cooling times between 50°C and 100°C of 32 seconds and 101 seconds, respectively. A Bluetooth enabled smartphone application has been developed for real-time data visualization. The utility of the temperature control system was shown by monitoring rhodamine B fluorescence in a microfluidic device over a range of temperatures, and by performing a polymerase chain reaction (PCR) within a microscope. This temperature control system could potentially impact a broad scope of applications that require simultaneous imaging and temperature control.

INTRODUCTION

The development of Lab on a chip (LOC) technology has impacted and advanced fields from engineering to biology[1]. These technologies have contributed to the understanding of fluid motion and associated transport processes[2] and offer promising solutions to drug discovery and development by significantly reducing sample consumption among other factors[3]. LOC technology revolutionized chemical and biological analysis by miniaturizing experimental techniques such as cell growth and manipulation[4], single cell analysis[5], molecular diagnostics[6-8], and complex chemical reactions[9], including the polymerase chain reaction (PCR) used for nucleic acid amplification. PCR is a powerful and sensitive technique used to quantify DNA and mRNA expression which has applications ranging from forensics to medical diagnostics[6,10]. These processes can now be performed on a device that fits on a standard microscope slide, which manipulates picoliter to microliter volumes of liquid[11,12] using microchannel dimensions ranging from tens to hundreds of microns. Small volumes enable massively parallel experiments[13,14] and allow multiple operations to be integrated onto one device[15]. The microfluidics industry is currently in the spotlight, as new LOC technologies could help curb pandemics through enhanced diagnostics and drug discovery[16]. For this reason, a significant growth is expected for the microfluidic diagnostic industry due to the immediate demand for global healthcare.

While the miniaturized format of LOC technology is highly advantageous, these dimensions frequently require a microscope or specialized imaging equipment to monitor experiments. Many of these operations, such as cell growth[17], chemical reactions and kinetic measurements[18,19], microfluidic mixing experiments, or biochemical reactions such as polymerase chain reaction (PCR)[20], additionally require precise temperature control, leading to the challenge of integrating temperature control into microfluidic systems.

Both external and internal heating techniques such as preheated liquids, microwaves, lasers, chemical reactions and Joule heating have been used on microfluidic devices for temperature control[7]. Many microfluidic temperature control systems are designed and fabricated with at least one component that is limited to a particular device design[15,21-25]. Thus, this prevents these temperature control systems to be used for more than one microfluidic design. While these systems provide

rapid thermal cycling or localized heating of a reaction chamber, these experiments require extra fabrication steps to integrate thermal control for every device or are not suitable for arbitrary device designs.

A thermal cycler with a large attached optical system has also been reported, which provides fluorescent images of microfluidic devices, but it includes a full sized commercial thermocycler and it cannot be used within a standard microscope[26]. Conversely, an inexpensive and portable thermal cycler with imaging capabilities was reported, but it does not integrate with a microscope and is therefore not intended to image small feature sizes[27]. Current commercial temperature control instrumentation for microscope stages can produce a steady temperature for the entire microscope stage; for example, the Microscope Temperature Control Heating Stage, Slide Warmer by BoliOptics provides whole-stage temperature control. However, they have a slow temperature acquisition rate and a narrow temperature range, as they were mainly designed for the purpose of cell culture. Another recent commercial device developed for fast temperature acquisition and control is the VAHEAT by Linnowave, but it is limited to a small temperature control region and is expensive. Linkham provides a peltier-cooled system with a broad working range (-25°C - 120°C) over approximately half of a microscope slide with 0.1 – 20°C/s heating and cooling rates. This instrument includes a large water pump to cool the peltier, however, and cannot be used when imaging under a microscope slide is required, such as during epifluorescent microscopy. While these advances have been an exciting addition to the field of microfluidic temperature control, there are currently no available inexpensive, modular, versatile instruments that can fit securely within most microscopes, operate during imaging steps, and uniformly control over a wide range of temperatures on any sample secured to a standard microscope slide.

To address these issues, we present an inexpensive system for simultaneous temperature control and imaging. The system can uniformly heat or cool any sample that can fit on a standard microscope slide, allowing simultaneous temperature acquisition and control as well as visualization of the sample. The system is divided into two main components: 1) The Device Holder, which is a stereolithography (SLA) 3D printed component that serves as a housing for the microfluidic device, the cooling fan, and the heating element and 2) The Control Device, which encloses the power supplies, the electronics, and the microcontroller. Powering the system requires only a single connection to the standard 120V wall power and can be programmed using a simple interface on the Control Device. The Device Holder is temperature resistant and can be removed from the electronic components, so it can be sterilized by autoclaving at the end of every experiment. The accuracy and uniformity of the temperature control was validated using an external thermometer and an IR camera. The functionality of the temperature control system was validated by monitoring temperature sensitive rhodamine B fluorescence in a microfluidic channel, as well as amplification of cDNA on a microscope slide within a microscope stage. Finally, a mobile application has been developed to plot temperature data in real-time, which is sent via Bluetooth connection from the Control Device to a smartphone. This temperature control system can be used on any device or sample that fits on a standard microscope slide. Therefore, it has the potential to enable the experiments involving live cell imaging, nucleic acid and protein analysis, *in vitro* drug studies, diffusion studies, crystallization, material characterization, microfluidic fluid mechanics; or any other application in which temperature control and simultaneous microscopic observation are required. Therefore, this temperature control system has implications for a broad scope of applications that require concurrent imaging and temperature control.

MATERIALS AND METHODS

3D design of the Device Holder and Control Device

The Device Holder incorporates the microscope slide or microfluidic LOC device with all heating and cooling components and fits securely on a microscope stage. In the presented design, all components that surround the microfluidic sample (figure 1a ii) are symmetric to avoid temperature gradients. The presented system is designed for epifluorescent microscopy, but imaging the top of the device could also be achieved without active cooling if the sample and the aluminum plate (figure1a iii) are flipped and the fan (figure 1a v) is removed.

The Control Device case was designed to enclose all the electronic components, such as the microcontroller and power supplies, to provide an accurate temperature control and to interface with the user (figure 1b and d). Both designs were drawn using SolidWorks (Waltham, MA).

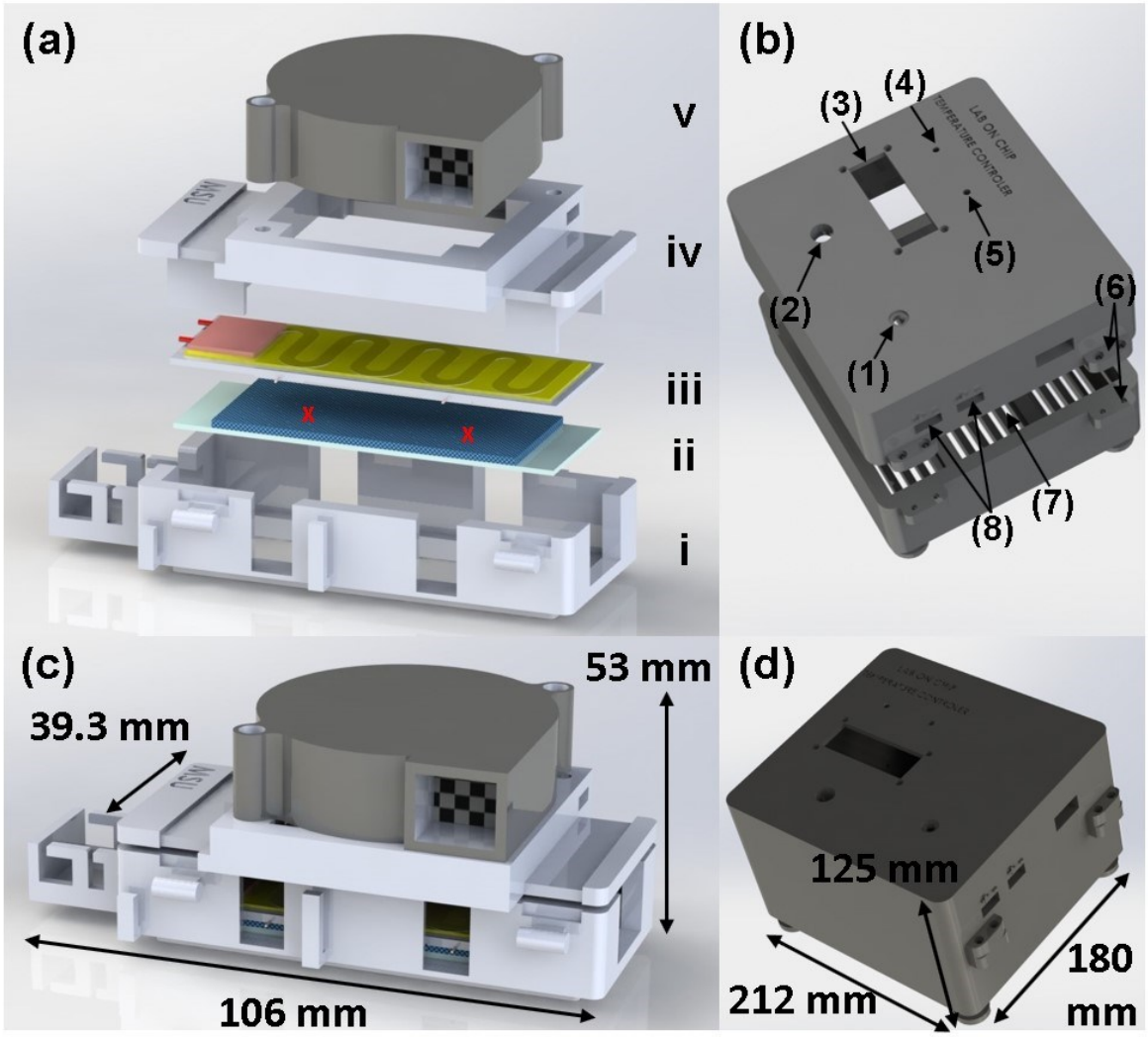

Figure 1. Schematics of the temperature control system: (a) CAD design of the experimental Device Holder, LOC device, and the heating and cooling components which fit into the microscope tray. (i) Lower part of the Device Holder. (ii) LOC device, which here is shown as a 1.5 mm thick microfluidic device layer bonded to a standard microscope slide. The thermocouples were placed between the aluminum heater and the device, with two red X's showing their approximate location. (iii) Heating Unit bonded to an aluminum sheet. (iv) Upper cap of the Device Holder. (v) Fan. (b) CAD design of the of the Control Device case for the microcontroller and all the electronical components used to create the interface of the Control Device. Shown here are the positions of the (1) Rotary encoder. (2) 6 pin connector for Device Holder linkage. (3) LCD display screen. (4) Green LED. (5) Yellow LED. (6) Couplings for the screws. (7) Ventilation slots. (8) Two type K thermocouple connections. (c) CAD design of the assembled experimental Device Holder with dimensions. Small white protrusions on the heater show the locations of the thermocouple wires, which fit through the slots on the side of the Device Holder. (d) CAD design of the assembled Control Device case with dimensions.

Fabrication of the Device Holder

The Device Holder incorporates a device or microscope slide with the cooling and heating unit. The breakdown of the components is shown in Figure 1a, the assembled Holder is shown in Figure 1c, and the final Device Holder prototype is shown in Figure 2. A Formlabs (Somerville, MA) Form 2 SLA 3D printer and High Temp Resin (RS-F2-HTAM-02) was used to fabricate the Device Holder (figure 1a, i and iv). The final design, including all the components, was 106x53x39.3mm. The Device Holder fits into the stage of the microscope and is secured by notches on the bottom of the holder. An Adhesive Polyimide Insulated Flexible Resistance Heater (OMEGA^{TM}, Norwalk, CT) was adhered to an aluminum sheet to create the heating module (figure 1a, component iii) and a 12Volt fan (WINSINN, Shenzhe, Guangdong) constitutes the cooling module. The pressure sensitive adhesive on the heater is rated for temperatures between -40ºC to 149ºC. Special limits of error type K thermocouples (OMEGA^{TM}, Norwalk, CT) were adhered to the underside of the aluminum sheet in contact with the sample (figure 1a, between components ii and iii) and provide the feedback for temperature control. Two thermocouples were included to confirm that a temperature gradient did not occur during device development and to ensure continuous temperature measurements in the unlikely event that one thermocouple

malfunctioned. The thermocouples were 33.5mm apart and 20.75 mm from the end of the device on each side. ; the locations of the thermocouples are shown as red X's in figure 1a for reference. Flexible rubber clamps (Ceeyali, Shenzhe, Guangdong) create full contact between the aluminum sheet and the LOC device by clamping the top and bottom 3D printed Device Holder elements together (figure 1a, components i through iv). The estimated expenses for the Device Holder fabrication is $122.94 for the components and $12.42 for the High Temperature Resin.

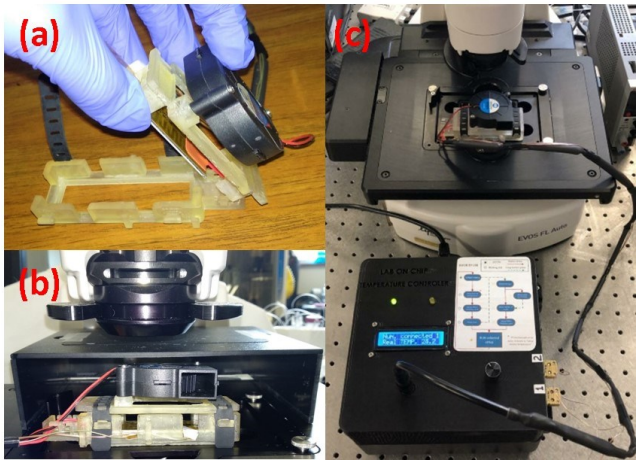

Figure 2. The Device Holder prototype. (a) Open Device Holder. (b) Clamped Device Holder within an epifluorescence microscope, which fits underneath a compact light shield. (c) Device Holder in a microscope with a connected Control Device.

Fabrication of the Control Device

The Control Device encloses all of the electronic components to control the device temperature and to interface with the user inside a case. The case design is shown in Figure 1b and d, and the entire Control Device prototype is shown in Figure 3. The case was 3D-printed using a Stanley Model 1 extrusion printer (Stanley Tools, New Britain, CT) and Prusa i3 MK3S (Prusa Research, Prague, Czech Re-public) with Sindoh 3DWOX Refill Black polylactic acid (PLA) filament. Figure 1d shows a schematic of the assembled Control Device casing, which is 212x180x125mm. The total estimated cost of the Control Device fabrication is $131.1 for the components and $52.4 for the PLA material.

The Control Device is connected into the electrical grid **(**wall power) and turned on using the green switch shown in Figure 3 component 5. Control is achieved using an Arduino ® Nano, which is located at the top of the Control Device next to the slot shown in Figure 3, component 8. The power supply is located below the controller, approximately 6 cm apart and separated by both a plastic mounting and an air gap. The heating unit is controlled using a Pulse Wave Modulation (PWM) coming from one of the power supplies incorporated in the Control Device for voltage regulation. The power supplies are currently configured for a 120 Volts AC conversion, but they could be adjusted for 220-240 Volts conversion. A fuse is incorporated into the system to open the circuit and stop the device operation in the case of electrical failure. An LCD screen is integrated into the Control Device to visualize the different menu options and real time temperature readings (figure 3, component 3). A rotary encoder is used to navigate through the eleven menu options (figure 3, component 2). In addition, one green LED and one yellow LED are used to help identify the menu option in which the user is positioned (figure 3, component 6). Two MAX6675 thermocouple temperature sensor modules from HiLetgo (Shenzhen, Guangdong) are used for cold-junction compensation and digitization of the type K thermocouple signal; details on the temperature calibration of the instrument are given in the Supporting Information (figure SI1). A user guide schematic is printed on the Control Device to help the user navigate through the menu and produce customized experiments (figure 3, component 4, and shown in more detail in figure SI2).

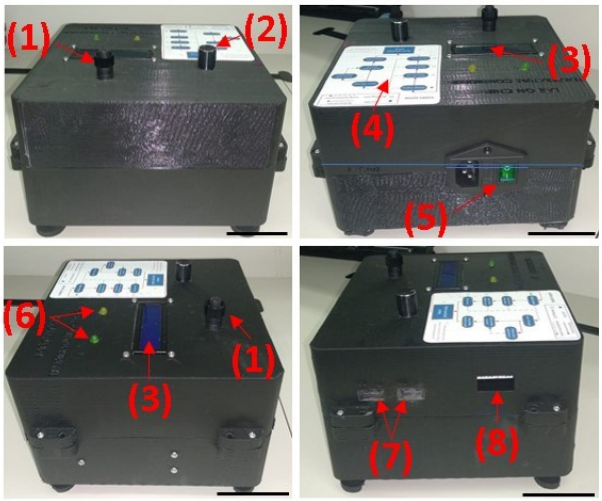

Figure 3. The Control Device: PLA black filament printed case with all hardware components needed for power conversion, parameter selection, visualization, and temperature control enclosed inside. (1) Device Holder to Control Device connection. (2) Rotary encoder. (3) LCD display screen. (4) User guide for menu navigation and device operation. (5) On switch. (6) LEDs indicating device operation. (7) Thermocouple connection slots. (8) USB 2.0 cable connection slot used to upload new experimental code. Scale bars are approximately 5 cm.

Temperature Control System software

The menus programmed into the microcontroller allow the user to customize an experiment by selecting the specific temperatures of the different steps, times, and number of desired cycles. The user can input the temperature control parameters either by modifying the Arduino-based code and uploading this into the Arduino microcontroller via the USB port (figure 3, component 8) or by using the rotary encoder on the top of the control device (figure 3, component 2). An example of the rotary encoder use is given in a supporting video. An additional input option to consider the microfluidic device thickness for internal device temperature inference was included for future applications but was not used in this work. The real time temperature is shown on the display of the Control Device (figure 3, component 3) and sent via Bluetooth to the LOC mobile application (figure SI2). Temperature data can also be monitored in the Arduino software when a computer is connected to the Control Device via USB. When both thermocouples are connected, the control temperature will be the average of both measurements. A gain

scheduling closed loop feedback PID control has been programmed based on the general equation of PID controller to regulate the duty cycle of the PWM. Thus, the optimal proportional, integral, and derivative were found using a trial and error procedure[28].

Smartphone application development

A smartphone application (app) was developed to acquire the real time temperature data of experiments performed with no need for the Arduino IDE. When the control has been activated through the rotary encoder in the Control Device and after the Bluetooth has been paired, the Control Device will send the temperature data via Bluetooth to the smartphone app. The temperature and time will be displayed as an integer value in a two-dimensional plot on the screen of the smartphone (figure SI3).

Rhodamine B temperature validation

Rhodamine B ≥95%, a temperature sensitive dye, was purchased in powdered form from Sigma Aldrich (St. Louis, MO), and a 10mM rhodamine solution was made in ultrapure MilliQ water. The PDMS microfluidic device was produced using standard soft lithography techniques and bonded to a glass microscope slide[29]. The rhodamine solution was pumped into the channels and wells of the PDMS microfluidic device using a syringe, and was covered by glass cover slip and mineral oil to prevent evaporation. The microfluidic device was inserted into the device holder and placed in the epifluorescent microscope oriented as shown in figure 1a. The temperature was varied by 5ºC increments during both heating and cooling, which was maintained for 5 minutes before measurement. Measurements were taken using the Evos Texas Red light cube and a 10x PlanFluor objective with a 0.3 NA (Thermofisher Scientific, Waltham, MA). Additional images were acquired using a Evos PlanFluor 0.45NA/20x objective to show that the device is compatible with a range of objectives (figure SI4), including a higher magnification. Illumination was constant throughout the course of the experiments. Average red fluorescent pixel values were evaluated using ImageJ[30]. Data were excluded from the analysis if evaporation occurred within the device.

PCR validation experiments

Reagents: Nuclease-free water was purchased from IDT (Coralville, IA). Cel-miR-39 mimic was purchased from Qiagen (Hilden, Germany). Luna® universal probe qPCR master mix and molecular grade bovine serum albumin (BSA) were purchased from New England Biolabs (Ipswich, MA). The cel-miR-39 TaqMan Assay and TaqMan microRNA Reverse Transcription Kit was purchased from Thermofisher (Waltham, MA). Molecular biology grade mineral oil and Sigmacote® were purchased from Sigma Aldrich (St. Louis, MO). Eliminase was purchased from Fisher Scientific (Hampton, NH).

PCR setup: The working stock was diluted to $9.6x10^7$ copies/µL in nuclease free water and cDNA was created using the TaqMan microRNA Reverse Transcription Kit according to manufacturer's instructions. PCR reactions contained 1µL 20x TaqMan small RNA assay reagents for cel-miR-39, 10µL Luna® universal probe qPCR master mix, 1 µL of 20mg/mL BSA, 1.2µL of cDNA, and 6.8 µL of nuclease-free water for a total of 20 µL. The negative control reaction contained a reverse transcription reaction performed with nuclease-free water instead of target miRNA. The final concentration of cDNA in the PCR reaction was theoretically $1.9x10^6$ copies/µL.

qPCR within the microscope:

A macrofluidic device was made by cutting two rectangular 10x6.5mm wells in a 0.2mm thick PDMS layer. The PDMS layer was bonded to a standard 1mm thick glass microscope slide (Globe Scientific, Mahwah, NJ) after exposure to oxygen plasma using standard PDMS bonding techniques. The exposed glass of the wells and a glass cover slide (22x50mm #1 thickness) (Thermo Scientific, Portsmouth, NH) were treated with Sigmacote® according to manufacturer's instructions. The device and the glass cover slide were rinsed thoroughly with milliQ water, then Eliminase, and finally nuclease free water.

A 1µL droplet of the positive sample was placed in one rectangular well and a 1 uL droplet of the negative sample was placed in the other rectangular well. The droplets were placed in the middle of the wells and immersed in mineral oil, and therefore did not contact the PDMS. Both wells were covered with approximately 8 µL of mineral oil. The glass cover slide was placed on top of the PDMS layer. It was observed that the PCR reaction could be inhibited if not sealed properly within the wells or if the droplets were fully in contact with the PDMS. Next, the macrofluidic device was placed in the Device Holder, approximately 50 uL of mineral oil was placed on top of the device and the Device Holder was closed, creating a thin film of oil between the aluminum heater and the glass. The device was then placed in the epifluorescence microscope. The thin oil film ensured contact between the heating element and the device and helped prevent evaporation of the aqueous phase. Thermal cycling was as follows: initial denaturation (91ºC for 4 minutes), followed by 40 cycles with two steps (91ºC for 15 seconds and 60ºC for 45 seconds). The total amount of time spent for the qPCR was 95.2 minutes (figure 7a). The macrofluidic device was imaged using an Evos FL Auto (Fisher Scientific, Waltham, MA) and an Evos 2x objective (0.06NA) with a GFP Evos light cube. Two positive and two negative samples (1 uL each and 9 uL of mineral oil) were loaded into a standard commercial thermal cycler CFX Connect (BioRad, Hercules, California) and subjected to the same thermal cycling steps as described above. ImageJ[30] was used to find the pixel intensity of green fluorescent light within a 75-pixel diameter circle in the center of the droplet in the fluorescent microscope images. The mean pixel intensity of the droplet during the 60˚C stage was baseline corrected using cycle 1 and normalized to the fluorescence of the positive sample during cycle 40. To compare the droplets in the device to those in the CFX Connect, baseline corrected data from the CFX Maestro software was also normalized to the fluorescence of the positive sample during cycle 40.

RESULTS AND DISCUSSION

Analysis of temperature control performance

Analysis of the temperature control was performed in a temperature range that is standard during chemical and biochemical experimentation. One example is the ubiquitous PCR; temperature and time of PCR cycles and steps depend on the chosen chemistry and target length, but most PCR cycles require temperatures between 50ºC and 100ºC[31]. The performance of the

temperature control system was therefore analyzed in this temperature range (figure 4). The maximum temperature difference between the two thermocouples was 1.8ºC and 2.3ºC during the heating and the cooling, respectively. The average temperature difference between the thermocouples was 1.4ºC during heating and 0.9ºC during cooling, which does not exceed the type K thermocouple standard limit of error of ±1.1 ºC (2.2ºC maximum difference) given by the manufacturer; the maximum deviation between the thermocouples during cooling only exceeds this expected error range by 0.1 ºC. The average numerically calculated heating rate within the PCR working range was 1.5 ºC/seconds, and the temperature of the aluminum sheet increased 50ºC in 32 seconds (figure 4a). The average numerically calculated cooling rate within the PCR working range was 0.5ºC/second, and the temperature of the aluminum sheet decreased by 50ºC in 101 seconds (figure 4b). Figure SI5 shows the temperature stability in the device at steady state, with 89.9% and 92.3% of the temperature points within ±0.3°C of the average temperature at 60°C and 91°C, respectively.

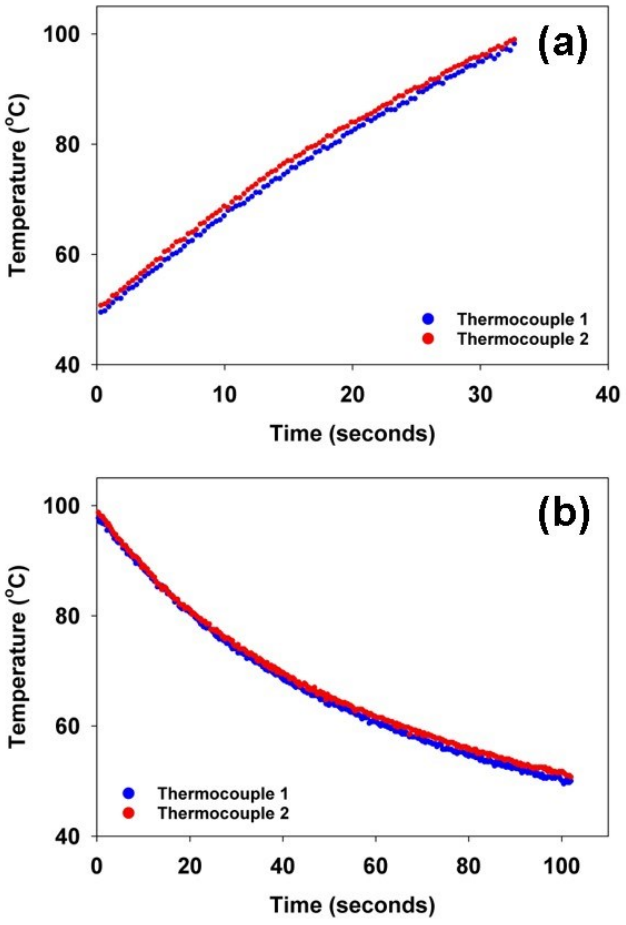

Figure 4. Heating and cooling rates. (a) Monitoring of the heating behavior. (b) Monitoring of the cooling behavior. The average difference between the thermocouples is 1.4°C during heating and 0.9°C during cooling, which is within the standard special limits of error for the incorporated type K thermocouples.

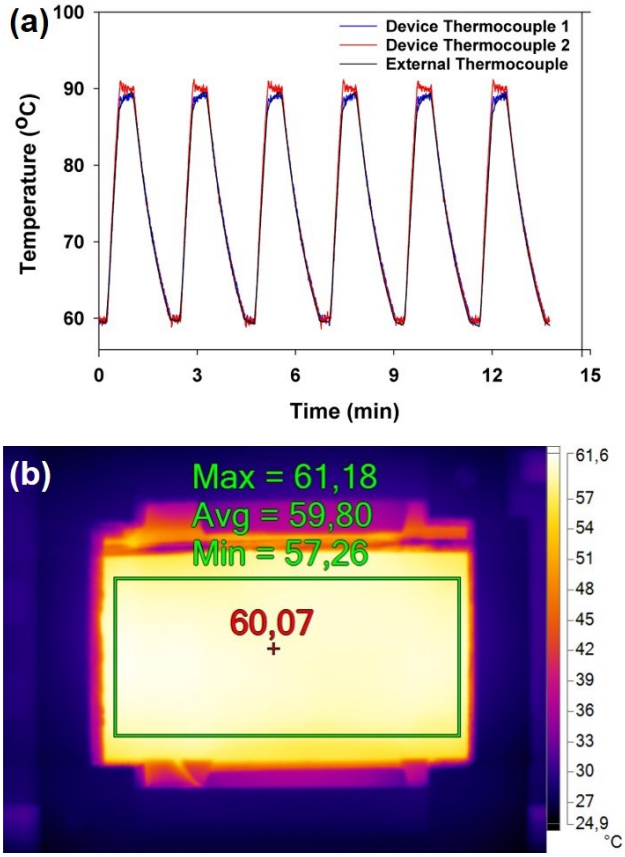

Figure 5. External validation of temperature accuracy. a) Temperature measurement at the base of the microscope slide bonded to PDMS for an arbitrary set of PCR cycles. The temperature is read from both type K thermocouples incorporated in the device and an external type K thermocouple. B) Thermal image taken with FLUKE TiX560 (Everett, Washington) of a glass microscope slide inside the device holder programmed to maintain a temperature of 60ºC. The cross indicates a temperature of 60.07ºC.

External validation of temperature control

The temperature controller system output was validated by tracking the temperatures over time both within the system and on an external analog thermometer. An external type K thermocouple connected to a SensorDAQ (Vernier, Beaverton, OR) was placed at the center of the device. The SensorDAQ readout was acquired using LabVIEW (National Instruments, Austin, TX). The Device Holder was assembled with a macrofluidic device and placed within the microscope as shown in figure 2a. The temperature from each thermocouple during a set of arbitrary temperature cycles (90 ˚C for 25 seconds, 60 ˚C for 15 seconds) is shown in figure 5a, with the externally measured temperature comparable to the temperature measured by the device. The temperature remained stable during each cycle at every measurement point. Additionally, the temperature at the surface of a glass slide was validated using a TiX501 thermal camera (Fluke, Everett, WA) to show uniformity of temperature across the top of a glass substrate (figure 5b) using an emissivity of 0.95[32].

Rhodamine B temperature dependence measured inside a PDMS/glass microfluidic device

Rhodamine B is frequently used to evaluate temperature in microfluidic devices based on fluorescent signal intensity ratios for temperature distributions[33]. To demonstrate the functionality of the temperature control system, the fluorescence of rhodamine B was monitored over temperatures ranging from 30 ˚C to 70 ˚C. A characteristic drop in Rhodamine B fluorescence relative to the fluorescence at 30 ˚C is seen with increasing temperature during both heating (n=1) and cooling (n=2) using two separate devices (figure 6). A broader temperature range typically requires a nonlinear polynomial fit[34], but for the (30-70 ˚C) temperature range shown in figure 6 a linear fit was suitable (R^2 = 0.99). This confirms the system can control temperature in a microfluidic device during fluorescent microscopy measurements.

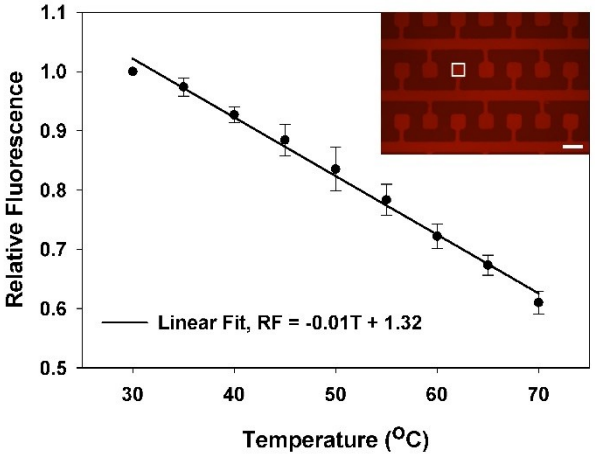

Figure 6. Average relative fluorescence change of rhodamine B in a microfluidic device during heating and cooling. The white square in the inset of the representative image of Rhodamine B is a dead-end filled microfluidic well (70 ˚C) which shows the area where the average fluorescence was taken. Error bars show ± one standard deviation for n=3 measurements. Scalebar = 100 μm.

qPCR amplification within the temperature control system

PCR amplification on droplets containing target cDNA and droplets without target cDNA was performed in a standard epifluorescent microscope in approximately 95.2 minutes (figure 7a). The macrofluidic device with a negative and positive control droplet was imaged during cycles 1, 5, 10, 15, 20, 24, 28, 32, 36, and 40. A histogram of the droplet pixel intensities for cycles 1 and 40 is also is shown in figure SI 8. An increase in the positive droplet fluorescence was observed between cycles 20 and 24, which matches the approximate time to positive seen in the BioRad commercial qPCR instrument (figure 7b). It is worth noting that the shape of the curve acquired from the microscope is not identical to the shape seen in the commercial qPCR instrument. This could be due to a variety of factors, such as interactions between the TaqMan chemistry and the hydrophobic Sigmacote; kinetic differences between PCR within custom devices and in optimized PCR tubes have been previously reported[27]. Figure 7 demonstrates that successful PCR amplification of reagents within a microscope can be achieved with the same approximate time to positive as a commercially available qPCR instrument.

Before running the real-time amplification, an additional end-point PCR experiment was successfully performed within the microscope stage. The figures and results are described in the SI (figure SI6 and figure SI7).

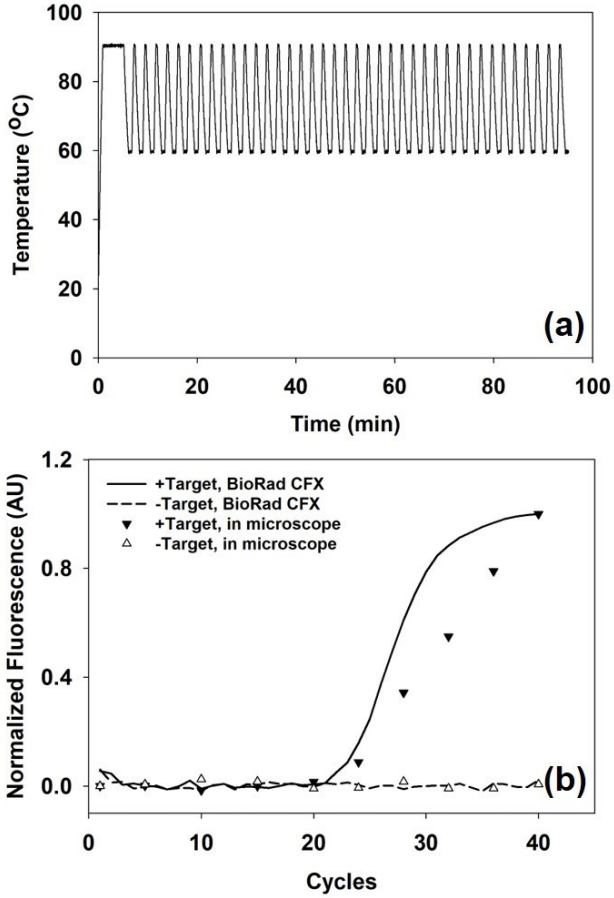

Figure 7. Real time PCR amplification using the temperature control system. (a) The temperature over the course of the real time PCR amplification, which was completed in 95.2 minutes. (b) Normalized fluorescence from 1μL droplets of PCR solution in a standard commercial qPCR instrument (lines) and using the temperature control system in a microscope (triangles). Open triangles indicate a sample with no target cDNA, closed triangles indicate a sample with target cDNA.

CONCLUSIONS

We have demonstrated and validated a compact, portable, modular, and user-friendly temperature control system that was created using an estimated budget of $318.86 without the benefit of production scale-up. It enables simple programming and control of temperatures on LOC devices or for any sample that fits on a standard microscope slide. The system precisely controls the temperature at the surface of a sample during imaging steps in an epifluorescent microscope. Temperature data can be displayed through a smartphone app and on the Control Device.

While the system does not require an attached computer to function, temperature data can also be collected on a computer through a USB connection to the Control Device if desired. The system was validated by an external thermometer as well as an IR thermal camera. In addition, the system temperature was monitored by measuring the fluorescence of the temperature sensitive dye Rhodamine B inside a microfluidic device. Finally, the system was tested by a successful initial-endpoint PCR and a real-time PCR amplification of a cel-miR-39 miRNA cDNA. The entire 40 cycle PCR, including the 4 minutes initial denaturation, occurred in 95.2 minutes.

While the temperature control system shown here is sufficient for many applications, including PCR amplification, users can easily modify the system according to their needs. If more accurate temperature control is required, the thermocouples could be replaced with more expensive RTDs, which have superior accuracy. Users can remove the fan, heat the bottom of the device, and image the device from the top during a constant temperature step; this would also allow the users to accommodate tubing to control flow during experiments. The instrument does have limitations: in its current form it cannot cool while imaging or lighting the sample from the top, nor can it accommodate tubing when heating the top of the device as performed in this work. The customizable nature of the system allows the user to manipulate the components based on the experiment requirements, however. This provides greater flexibility to end users and expands the potential applications of the temperature control system. The modular nature of the system also allows the user to easily replace the components if they become damaged.

The temperature control system described here is an inexpensive, portable, reusable, enabling technology with potential applications in chemistry, biology, physics, medicine, material science, and other industries that require concurrent imaging and temperature control.

ASSOCIATED CONTENT

Supporting Information

The supporting information (pdf) contains the following information: the user guide demonstrating how to navigate through the menus programmed into the microcontroller, an image of the cell phone application output, the methods, materials and results for one end-point PCR as well as additional results for the real-time PCR performance, thermocouple calibration data of the system, additional images of microfluidic devices during heating, and details on thermal stability of the device at constant temperatures..

The Supporting Information is available free of charge on the publication website.

AUTHOR INFORMATION

Corresponding Author

*stephanie.mccalla@montana.edu

Author Contributions

P.M.C. Designed and developed hardware, software and 3D parts of the device, performed experiments, and prepared the manuscript.
M.W. Performed validation experiments, calibrated thermocouples, and prepared the manuscript.
R.A. Setup and ran 3D-printers, edited the manuscript.
T.B.L. Advised on 3D-printing, edited the manuscript.
S.E.M. Acquired funding, designed experiments, and prepared and edited the manuscript.

ACKNOWLEDGMENT

This material is based upon work supported by the National Science Foundation under Grant Number 1847245 and Grant Number 1736255. We thank the Wilking lab at Montana State University for use of their 3D printers. We acknowledge the Fluke corporation for their donation of a thermal imaging IR camera.

REFERENCES

(1) Reyes, D. R.; Iossifidis, D.; Auroux, P.-A.; Manz, A. *Analytical chemistry* **2002**, *74*, 2623-2636.

(2) Stone, H. A.; Stroock, A. D.; Ajdari, A. *Annu. Rev. Fluid Mech.* **2004**, *36*, 381-411.

(3) Dittrich, P. S.; Manz, A. *Nature reviews Drug discovery* **2006**, *5*, 210-218.

(4) Andersson, H.; Van den Berg, A. *Sensors and actuators B: Chemical* **2003**, *92*, 315-325.

(5) Dusny, C.; Grünberger, A. *Current opinion in biotechnology* **2020**, *63*, 26-33.

(6) McCalla, S. E.; Tripathi, A. *Annual review of biomedical engineering* **2011**, *13*, 321-343.

(7) Miralles, V.; Huerre, A.; Malloggi, F.; Jullien, M.-C. *Diagnostics* **2013**, *3*, 33-67.

(8) Jung, W.; Han, J.; Choi, J.-W.; Ahn, C. H. *Microelectronic Engineering* **2015**, *132*, 46-57.

(9) Kaminski, T.; Garstecki, P. *Chemical Society Reviews* **2017**, *46*, 6210-6226.

(10) Bruijns, B.; Van Asten, A.; Tiggelaar, R.; Gardeniers, H. *Biosensors* **2016**, *6*, 41.

(11) Zheng, B.; Roach, L. S.; Ismagilov, R. F. *Journal of the American chemical society* **2003**, *125*, 11170-11171.

(12) Beer, N. R.; Hindson, B. J.; Wheeler, E. K.; Hall, S. B.; Rose, K. A.; Kennedy, I. M.; Colston, B. W. *Analytical chemistry* **2007**, *79*, 8471-8475.

(13) Srivannavit, O.; Gulari, M.; Hua, Z.; Gao, X.; Zhou, X.; Hong, A.; Zhou, T.; Gulari, E. *Sensors and Actuators B: Chemical* **2009**, *140*, 473-481.

(14) Geertz, M.; Shore, D.; Maerkl, S. J. *Proceedings of the National Academy of Sciences* **2012**, *109*, 16540-16545.

(15) Burns, M. A.; Johnson, B. N.; Brahmasandra, S. N.; Handique, K.; Webster, J. R.; Krishnan, M.; Sammarco, T. S.; Man, P. M.;

Jones, D.; Heldsinger, D. *Science* **1998**, *282*, 484-487.
(16) Lamprou, D. A. *Expert review of medical devices* **2020**, 1-6.
(17) Chen, T.; Gomez-Escoda, B.; Munoz-Garcia, J.; Babic, J.; Griscom, L.; Wu, P.-Y. J.; Coudreuse, D. *Open biology* **2016**, *6*, 160156.
(18) Jähnisch, K.; Hessel, V.; Löwe, H.; Baerns, M. *Angewandte Chemie International Edition* **2004**, *43*, 406-446.
(19) Demello, A. J. *Nature* **2006**, *442*, 394-402.
(20) Woolley, A. T.; Hadley, D.; Landre, P.; deMello, A. J.; Mathies, R. A.; Northrup, M. A. *Analytical Chemistry* **1996**, *68*, 4081-4086.
(21) Casquillas, G. V.; Fu, C.; Le Berre, M.; Cramer, J.; Meance, S.; Plecis, A.; Baigl, D.; Greffet, J.-J.; Chen, Y.; Piel, M. *Lab on a Chip* **2011**, *11*, 484-489.
(22) Angione, S. L.; Chauhan, A.; Tripathi, A. *Analytical chemistry* **2012**, *84*, 2654-2661.
(23) Amasia, M.; Cozzens, M.; Madou, M. J. *Sensors and Actuators B: Chemical* **2012**, *161*, 1191-1197.
(24) Bu, M.; Perch-Nielsen, I. R.; Sørensen, K. S.; Skov, J.; Sun, Y.; Bang, D. D.; Pedersen, M. E.; Hansen, M. F.; Wolff, A. *Journal of Micromechanics and Microengineering* **2013**, *23*, 074002.
(25) Kimura, Y.; Ikeuchi, M.; Inoue, Y.; Ikuta, K. *Scientific reports* **2018**, *8*, 1-10.
(26) Selck, D. A.; Ismagilov, R. F. *PLoS One* **2016**, *11*.
(27) Mendoza-Gallegos, R. A.; Rios, A.; Garcia-Cordero, J. L. *Analytical chemistry* **2018**, *90*, 5563-5568.
(28) Wade, H. *InTech* **2005**, *52*, 38-42.
(29) Duffy, D. C.; McDonald, J. C.; Schueller, O. J.; Whitesides, G. M. *Analytical chemistry* **1998**, *70*, 4974-4984.
(30) Schneider, C. A.; Rasband, W. S.; Eliceiri, K. W. *Nature methods* **2012**, *9*, 671.
(31) Klein, D. *Trends in molecular medicine* **2002**, *8*, 257-260.
(32) Schweiz, M. V. *Schaffhausen: Mikron Instrument, nd Print* **2012**.
(33) Shah, J. J.; Gaitan, M.; Geist, J. *Analytical chemistry* **2009**, *81*, 8260-8263.
(34) Fu, R.; Xu, B.; Li, D. *International Journal of Thermal Sciences* **2006**, *45*, 841-847.